An Experimental Evaluation of Tribological &Morphological Excellence for LTB Alloys

Ram Dhani Chauhan [1] *, Dr. Prem Kumar Bharti [2]

[1] *Research Scholar, Department of Mechanical Engineering, Integral University, Lucknow, India*
[2] *Professor and Head, Department of Mechanical Engineering, Integral University, Lucknow, India*
*Corresponding author E-mail: rdc9100@gmail.com

Abstract

LTB(leaded tin bronze) alloys are popular for bush bearing, impeller, and sand guard of submersible, HSC(half split casing), and end suction centrifugal pump sets. Morphological study by OEM(optical emission microscope) of sand-cast different composition mixed LTB alloys shows that the percentage of Sn element in the composition is a deciding factor for the appearance of α, ß &δ phases in the copper matrix. α-phase formation will occur up to wt.8%of Sn, α phase formation with nucleation of ß phase occurs between 8-9% of Sn, ß phase occurs for 9-12% of Sn, ß phase with nucleation of δ phase occurs after 12% of Sn, and significant δ phase is visible at 14.5% of Sn. The hardness of LTB alloys increases with the addition of Sn%, provided that the increment of Pb% works as a softening agent between 3.5-14.5% of Sn. The developed hardness model for BHN (Brinell Hardness Number) of LTB alloys has performed well, with an average error of ±9.5%. The highest wear resistance was found as 3.89x10⁻3 gm/m and COF of 0.505 at 1500 rpm and 50 KN normal load for LTB6 alloy.

Keywords: *LTB (Leaded Tin Bronze); Morphological Study; Hardness; Grain Boundary; α Phase; ß Phase & δ Phase; COF (Coefficient of Friction); Wear Resistance.*

1. Introduction

Good castability, corrosion resistance, low friction, good wear resistance, high thermal and electrical conductivity, and good mechanical qualities at ambient and elevated temperatures are all attributes of copper alloys. Leaded tin bronze (LTB), tin bronze, phosphor bronze, and aluminium bronze are some names for copper alloys. Its alloy nomenclature depends on the copper matrix's leading percentage of alloying elements like Tin, phosphorus, or Aluminium. In short, aluminium bronze is denoted as AB, Phosphorus bronze as PB, & Leaded bronze as LB. LTB is a type of bronze alloy that usually contains Sn (3-15%), Lead (1-25%), Zn (0-5%), Ni (0-2%), and copper (75 - 90%) with minor variation in each wt.% of component. LTB has the properties of good castability, Low frictional coefficient, high wear and corrosion resistance, and high thermal conductivity. Because lead forms as a lubricating film to lessen friction and wear on bronze, leaded bronze is one of the most commonly utilised copper alloys in bearings. Researchers are drawn to studying alloys' tribological characteristics for their solid lubrication and hardness since wear and friction cause mechanical components to fail and dissipate energy [1-4]. The shore D hardness values of PA6(polyamide) and PA6GF25(polyamide and glass fibre) were 75.11 and 83.93, respectively, by Zaghloul et al. [3], which indicates that alloying more wt.% of rigid and more complex components in the matrix will enhance the hardness of alloys. According to Zaghloul's authentication, the size, type, volume percentage, and adhesive strength of the fibres in plastic-fibre composites determine the composite's hardness [5]. Friction-induced energy losses account for a larger portion of the economy, particularly in the transportation sector (85%), the industrial sector (45%), and residences (45%) [6].

LTB alloys are used primarily for bearings/ impellers/bushings of submersible pumps for moderate to high load and speed. The hardness of AB, PB, and LTB occurs like AB> PB >LTB. Tensile properties and hardness of permanent mould casting, centrifugal casting, and continuous casting are better than sand mould casting since they produce finer and denser grain structure than sand casting. Lead exists in copper alloys as discrete globules, which guard against seizure in dry lubrication. Tin bronze has excellent corrosion resistance, reasonably high tensile strength, and good wear resistance. These are primarily used in sleeve bearings and are found well against the Steel family. Because of its softness, lead weakens tin bronze bearing alloys, but it can also withstand situations involving interrupted lubrication. To preserve the journals, lead also permits dirt or foreign objects to attach themselves to the bearing surface inadvertently. Copper is a straightforward metallurgical material with a single face-centred cubic α phase that solidifies at a set temperature of 1080 degrees Celsius. Tin increases the copper matrix's strength and resilience to aqueous corrosion by forming an intermetallic combination with Cu and Sn. Deyong et al. [7] have investigated Cu-Sn-Ni alloy, where for a fixed wt.% of Ni, as the wt.% of Sn increases, the hardness of the bronze alloy increases. Pb solidifies only after the casting has cooled to 700 degrees centigrade. The lead segregation at last to solidify is therefore a potentially serious problem. The heat treatment of nickel-tin bronze could be done to produce precipitation hardening. The

precipitation phase of Cu-Sn is a copper-tin intermetallic compound that forms during slow cooling in moulds or subsequent ageing treatment.

In addition to the fact that lead, nickel, and tin-based bronze are not regarded as heat treatable, lead is not appropriate for the hardening process. Although the freezing range increases slightly with increasing nickel concentration, the copper-nickel consolidated over minimal freezing ranges. Ni segregation in copper and nickel-rich phases is not a significant issue. As a result, the copper-nickel system is a metallurgically simple alloy made up of a continuous series of solid solutions. Lead segregates into tiny liquid pools as lead copper alloys freeze, filling and sealing the interdendritic microporosity after the higher melting elements solidify. The alloys are also free-cutting due to Pb. Lead-containing copper alloys can be brazed and soldered, but cannot be welded.

Rahul Gupta et al. [8] assessed the tribological characteristics of high-leaded tin bronze with grain refinement sizes ranging from 120 nm to 37 nm. This work examines wear rate and microstructure-related mechanical property changes during "MDF (Multi-Direction Forging)" of high-leaded tin bronze alloy, as indicated in Table 1.

Table 1: Chemical Ingredients of Bronze Alloy (wt.%)

Cu	Sn	Ni	Sb	Zn	P	Fe	As	Bi	Pb	Si	Al	Mn
69.766	5.004	0.63	0.25	3.52	0.02	0.2	0.03	0.003	20.58	<0.001	<0.001	<0.001

This study discovered that increased MDF passes considerably raises the alloy's hardness. It was found that the alloy's hardness was elevated from 63 HV for the undeformed sample to 146Hv for the 9MDF passes, or around 131% higher than the hardness of the undeformed sample. The Hall-Petch equation has been used to describe the strengthening as well as hardening caused by grain refining, $\sigma y = \sigma 0 + KD^{-1/2}$, and $Hv = H0 + KD^{-1/2}$, where yield strength σy and room temperature hardness Hv are inversely proportional to the material average grain size (D) (Xiang et al. [9])

It was determined that the wear rate on MDF alloy was reduced by increasing the sliding speed. Prasad also saw a similar pattern using leaded tin bronze [10]. The higher wear rate does occur due to the smaller speed range (0 to 0.35m/s) as compared to the bigger speed range (0.40-0.8m/s). It may have occurred because the reduced speed of 0.35m/s is not conducive to forming a lead layer on the mating surface. According to Pathak et al. [11], the lead particle layer acts as a solid lubricant between sliding surfaces due to the increased heat production at higher speeds, which could be the reason for the reduction in wear rate at high speeds. The impact of the decline in wear rate with hardness for bearing alloys is explained by the Archard law (Gao et al. [12]), which states that $Q = KLN/H$. Here, Q denotes volume loss inversely related to H (hardness) of the wear surface, L denotes total sliding distance, N denotes applied normal load, and K denotes wear coefficient.

According to research by Moustafa et al. [13], copper-coated graphite outperformed noncoated copper-graphite in terms of wear rate and coefficient of friction in copper-graphite composites with a volume proportion of 0–20% graphite. Rajkumar et al. [14] showed that microwave-sintering copper-nano graphite composites increased load-bearing capacity, lowered wear rate, and frictional value. According to experiments conducted by S. IlanGovan et al. [15], a dendritic structure was discovered in the solid solution of Sn in the base material copper. The dendritic structure was observed to be removed following homogenisation and solution heat treatment (heating for one hour at 820°C and quickly quenching in water). Zhang et al. [16] and Singh et al. [17] observed precipitation of Sn in the grain boundary following heat ageing (350 ^{0}C, 1 to 5 hours).

The secondary dendrite arm spacing (SDAS) is inversely related to the ultimate tensile strength of the cast sample LTB, and its fraction percentage increases as the cooling rate increases [18,19]. Due to grain refinement, a higher cooling rate enhances the strength of the cast product. For 80% Cu-20% Sn, Sugita et al. [20] observed that as the solidification rate during casting increases, the hardness of the tin bronze alloy improves with finer grain refinement. Dispersion strengthening, grain size refinement, solid solution or quench hardening, strain hardening, and precipitation hardening contribute to improving material strength [21]. Because of their extensive applications, bronze alloys are vital in the petrochemical, energy, military, transportation, manufacturing, and metallurgical sectors [22].

Traditionally, a bronze alloy comprises twelve percent tin and eighty-eight percent copper. However, additional metals that involve phosphorus, zinc, nickel, and aluminium are rarely added to enhance their qualities [23]. All bronze alloys share strong ductility, low friction against different metals, and corrosion resistance, though their specific characteristics vary based on their composition and manufacturing method [24].

The leaded-tin bronze, the subject of this study, is relatively strong, complex, and highly resistant to wear. Copper and tin alloys are known as tin bronzes. Zinc is also added to tin bronzes to enhance the alloy's running properties during castings. Lead and tin are present in leaded-tin bronzes, which are frequently employed in bearing applications different from tin alone in tin-bronzes.

Bronze, an alloy of Copper and Tin, has been known since 2500 BC. The contemporary need in the present Era is to find out the optimum composition of alloying elements to get better wear resistance and COF (coefficient of friction) to reduce the pollution and consumption of raw material for the sustainability of the environment. Researchers have coined the term green tribology, which focuses on reducing the wear cost of components used in machinery for industrial, agricultural, or domestic purposes. Pb and graphite are the most common solid lubricants in the copper matrix due to their good tribological and mechanical properties.

2. Methodology and Experimental Details

The sand casting method was used to cast different samples of LTB alloys. It´s a predecided composition mix for different samples, i.e., LTB1-LTB12 was poured into the crucible sequentially. This crucible was heated in a pit furnace up to 1200°C °C, as shown in Fig.1. Precaution like complete stirring of the molten alloy was taken before pouring into a sand mould for samples. Castings of samples were cooled at atmospheric temperature for 24 hours, and then machined the cast samples as shown in Fig. 2. The chemical analysis, morphological study, and hardness testing were completed by various methods like OES (optical emission spectroscopy -Spark, Arun Technology Poly Speak-F), OEM (optical emission microscope, Carl Zeiss, Test method- ASM Handbook Vol 9-2004), and Brinell Hardness Tester, respectively. For repeatability of the test result, three sets of readings (27 sets of readings for 09samples) were taken for BHN evaluation, then averaging was done. Regression analysis was used for hardness model development based on experimental hardness values. The Student-T-Test was used to assess the model's authenticity for a confidence limit of 5%. Wear, and COF (coefficient of friction) test of LTB alloys was conducted on Pin-on-Disc Tribometer with fixed technical parameters as normal load-50 KN, speed-1500rpm, disc material-EN31, and time of run-15 minutes. The test was conducted without lubrication.

Fig. 1: LTB in Molten State in Pit Furnace.

Fig. 2: LTB Sample.

2.1. Physical properties of LTB alloys

The solid solution of LTB alloys has different alloying elements like Sn, Pb, Ni, and Zn with Cu as the matrix. The solubility of different alloying elements may also be affected by their atomic size and lattice structure. Hence, the physical properties of LTB components are given below in Table 2.0, along with their physical appearance.

Table 2: Physical Properties of LTB Components

S. N	Chemical element and physical appearance	Atomic No	Density g/cm³	Melting Point ^{0} °C	Boiling Point 0 °C	COF	Crystal structure	Hardness HB
I	Cu	29	8.96	1085	2560	0.8-1.2	Face-centered cubic (FCC)	80-90
II	Pb	80	11.34	327	1749	0.6-0.9	FCC	38-55
III	Sn	50	7.29	231	2602	0.4-0.6	Tetragonal	15-20
IV	Ni	29	8.90	1455	2913	0.5-0.8	Face-centered cubic (FCC)	65-85
V	Zn	30	7.14	419	907	0.4-0.6	Hexagonal Close pack (HCP)	40-60
VI	Gr	Crystal of Carbon (6)	2.26	3825	3825	0.05-0.1	Hexagonal (Trigonal)	1-2

Copper in the Alpha phase of bronze casting is produced by slow solidification, whereas copper in the Delta phase is produced by rapid cooling. Tin in bronze has a minor impact on copper's thermal conductivity but boosts the alloy's strength. When zinc is added to copper, zinc deoxidises the casting and eliminates blow holes. Zinc will keep the Pb distribution uniform in a bronze alloy with strong corrosion resistance. Pb is very poorly soluble in liquid copper and almost entirely insoluble in solid copper or its alloy. Pb will accumulate between the Cu and Sn boundaries as irregular globules. The thermal conductivity of copper is unaffected by Pb's insolubility, according to Chauhan et al. [25]. In the alloy, it will function as the lubricant. A corrosive solution's resistance to corrosion will be improved by the presence of nickel in bronze. A thumb rule guideline for choosing bush material is taken as priority order, like corrosion, then erosion, and lastly cavitation resistance. It might be denoted as CEC (corrosion, erosion, and cavitation in order of corrosion resistance>erosion resistance>cavitation resistance). To achieve excellent wear resistance and a low coefficient of friction, it is crucial to choose bronze with an appropriate composition % of Pb, Sn, Ni, and Zn, as discussed above.

2.2. Chemical analysis of samples

Samples of LTB alloys were cast by sand casting with different alloying components of various compositions. The chemical analysis was done by the OES method, and the findings of the weight percentage of each element are given in Table 3.

Table 3: Classification of Sample Composition

Sample numbers	Sn wt %	Pb wt %	Zn wt %	Ni wt %	Cu wt %
LTB1	3.5	15.36	0.06	0.9	79.88
LTB2	5.25	3.13	4.26	2.49	84.69
LTB3	6.51	4.01	0.92	1.89	86.30
LTB4	7.79	11.13	0.79	1.32	78.24
LTB5	9	16	0.11	1.65	72.46
LTB6	9.10	10.15	1.33	1.98	77.40
LTB7	9.16	4.53	0.98	3.80	80.60
LTB8	12.42	12.57	0.24	4.38	70.28
LTB9	14.52	11.85	1.51	3.36	68.24

From Table 3, it is clear that no ordered increment in component wt.% is visible. This is probably due to their density difference and the evaporation of molten components despite stirring during melting and before pouring into the sand mould.

2.3. LTB samples classification and their morphological analysis

Nine different samples of Bronze were made by sand casting, and they are classified as LTB1, LTB2, LTB3, LTB4, LTB5, LTB6, LTB7, LTB8, and LTB9 for experimentation purposes. The morphological study of lattice structure was done using a Carl Zeiss microscope with a magnification of 200X on a scale of 50 μm. The different compositions of LTB alloys have shown different morphological structures, which are enumerated below in Figs3,4,5,6,7,8.
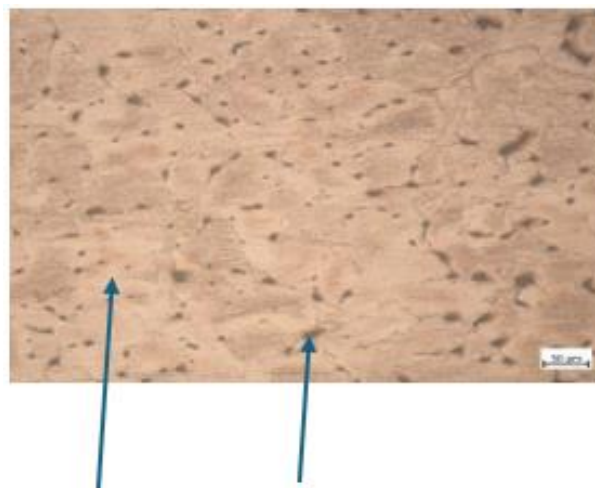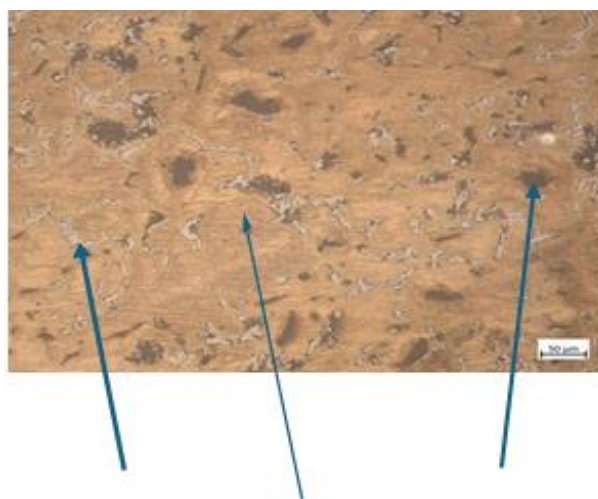

α phase (Cu rich) (Pb rich)

Fig. 3: Sample LTB1.
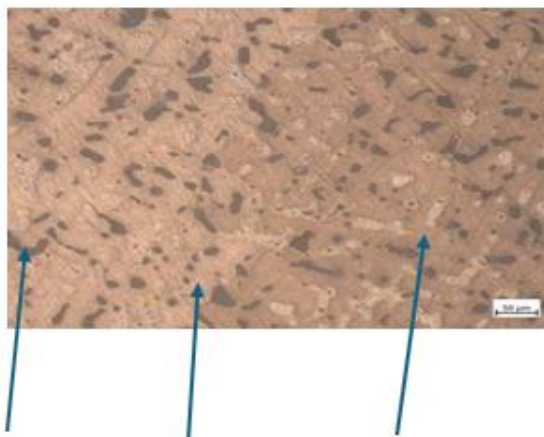
(Pb rich) ß phase (Sn rich) (α phase Cu rich)
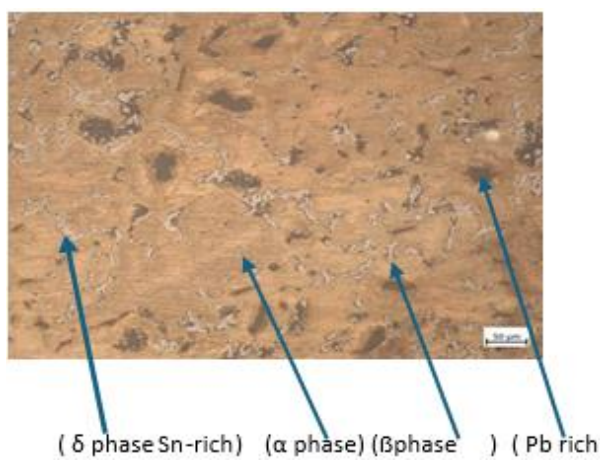
Fig. 4: Sample LTB4.

(ß phase Sn-rich)   (α phase)   (Pb rich)

Fig. 5: Sample LTB 5.

(ß phase, Sn rich)   (α phase)   (Pb rich)

Fig. 6: Sample LTB6.

(δ phase Sn-rich)   (α phase) (ßphase   ) (Pb rich)
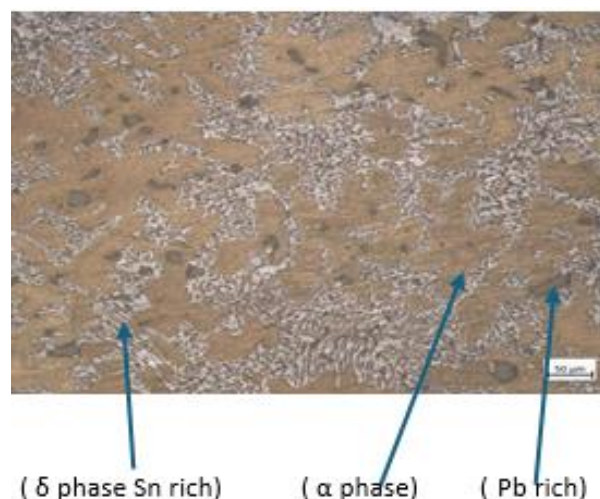
Fig. 7: Sample LTB 8.

Fig. 8: Sample LTB 9.

The above lattice structure images show that as a low percentage of Sn (up to 8%) in LTB alloy, the α phase (Cu rich) exists, while the Pb-rich phase exists on Grain boundaries. This is coherent with Wang et. Al[26], who has investigated Lead bronze (Cu-78.54%, Zn-0.03 %, Pb-15.35%, Sn-4.75%, and Ni-1.33%) and observed that the α phase exists with a soft Pb phase. In the Transition phase (Sn%8-9), Sn exists as a supersaturated solid solution with Cu matrix, but the inception of the ß phase (Sn-rich) appears, and Pb appears on grain boundaries. As the wt. The percentage of Sn increases beyond 9%, then explicit ß phase and α phase appear on the lattice structure image, while Pb-rich regions appear in the grain boundaries of the lattice. At 12% of Sn mixture in LTB alloy, α and ß phases coexist, but the inception of δ phase appears, and Pb-rich regions appear mainly in the lattice. At 14% of Sn or higher mixture in LTB alloy, α and δ phases (Lamellar structure) exist, and Pb-rich appears mainly in the lattice. α phase (copper-rich) is a Fcc structure and solidifies below 500 ^{0} C, while ß phase occurs between 600-800 ^{0} C. ß phase is a BCC structure and intermetallic compound of Cu and Sn, like Cu3Sn or Cu10Sn3. α and ß phases can coexist up to 12% of Sn. The ß phase has a denser pocket or lattice, which leads to higher hardness. The ß phase has a smaller grain size and ordered arrangement than the α phase of copper. The ß phase has higher electron density than the α phase due to more electrons from the Sn atom. The grain shape ofα looks cellular in structure, while the ß phase appears as a needle, rod, dendritic, or lamellar, with random orientation, coarse and dispersed. The presence of Pb appears as a globular-like structure, coarse and dispersed.

2.4. LTB samples hardness measurement

The BHN hardness of all samples 1-9 was measured as per IS:1500(P-1):2019. The readings obtained are shown below in Table 4 and as a bar chart in Fig. 9:

Table 4: Experimental Hardness of LTB Samples

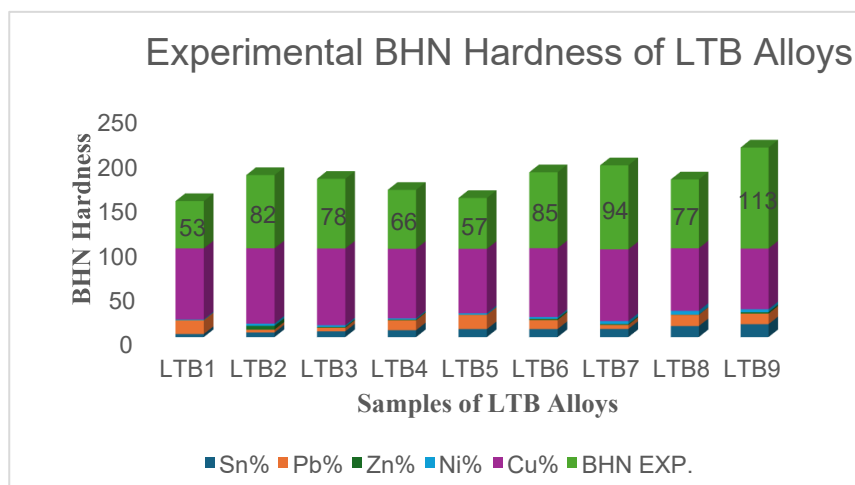| Sample numbers	Sn wt%	Pb wt%	Zn wt%	Ni wt%	Cu wt%	Hardness (HB)
LTB1	3.5	15.36	0.06	0.9	79.88	53
LTB2	5.25	3.13	4.26	2.49	84.69	82
LTB3	6.51	4.01	0.92	1.89	86.30	78
LTB4	7.79	11.13	0.79	1.32	78.24	66
LTB5	9	16	0.11	1.65	72.46	57
LTB6	9.10	10.15	1.33	1.98	77.40	85
LTB7	9.16	4.53	0.98	3.80	80.60	94
LTB8	12.42	12.57	0.24	4.38	70.28	77
LTB9	14.52	11.85	1.51	3.36	68.24	113

Fig. 9: Experimental BHN Hardness of LTB Alloys.

Based on the above reading, it is clear that as % of Sn increases, the Hardness of LTB alloys increases, but the presence of Pb contributes to the softness of alloys. Despite a higher percentage of Sn, if the value of Pb is higher than Sn, the hardness of the sample decreases. Hence, the alloying element Pb is working as a softening agent with the copper matrix. The interaction of Sn with copper makes an intermetallic compound like Cu3Sn, Cu6Sn3, or Cu6Sn5. In the α phase, Sn disperses in the solid solution of copper, while in ß and δ(HCP structure), Sn appears as precipitate in the grain or grain boundaries. This will impede dislocation movement; hence, hardness increases, and this adheres to the findings of S Ilangovan et al. [15]. This illustrates how hardening increases as the amount of Sn in solid solution increases, and the hardness model for Sn contributor is developed as H=15*Sn +176 (where the value of Sn is in wt. percentage). Similarly, Chauhan et al. [24] have analysed that Sn content increases from 0-100% (Cu-6%Ni4%Sn/Cu-6%Ni-8%Sn) as hardness elevates from 0 -26.1%. A. Sirinaidu et al. [27] have evaluated by experimentation that among the Bronze samples of Cu5Sn2Zn, Cu10Sn2Zn, and Cu12Sn2Zn, the hardness in terms of HRB was found as 30,60, and 80, respectively, which suggests that as the wt. Percentage of Sn increases, the Hardness of the Bronze increases. The atomic size of Pb is much higher than that of Cu, so it will be available as precipitate in grain boundaries. Zn, along with copper matrix, works as a hardening agent since it disperses as a solid solution, but when it alloys with copper in the presence of Pb and Sn, it will work as a softening agent. Ni dissolves in the copper lattice, creating a distortion that impedes dislocation movement, so this solid solution strengthening mechanism increases the alloy's hardness. Ni can form precipitates with other elements such as Cu, Sn, and Zn. Ni might be helping to refine the grain size of the alloy. This can lead to increased strength due to the Hall-Petch relationship, which is given below:

$$\sigma y = \sigma i + K/\sqrt{d}$$

Here, σy = yield strength of material, σi = yield strength of single crystal, K=hall patch coefficient d=average grain size
According to this relationship, yield strength rises as grain size falls. More grain boundaries can serve as obstacles to dislocation migration, which is why this occurs. The strength of alloys improves as the total number of grain boundaries increases.

2.5. Sn as a visible factor for a hardness enhancer

From the experimental values of LTB alloys' hardness, Sn contributes as a hardness enhancer in different forms, which are given below:

2.5.1. Solid solution strengthening

Sn dissolves in the Cu lattice, creating the solid solution. This dissolution leads to lattice distortion and Peierls stress. In lattice distortion, the Sn atom being larger than the Cu atoms creates a lattice distortion that impedes dislocation movement. Similarly, Peierl's lattice distortion increases Peierl's stress, creating further obstacles for dislocation movement. Beta phase of Tin in copper typically nucleates in grain boundaries, triple points, dislocations, and defects. Beta phase level can form globular, rod-like, and dendritic-like morphologies. Sn has almost a similar atomic size to Cu matrix, leading to mutual solubility, meaning that they can dissolve in each other to form a homogeneous alloy, with similar electronegativity, which reduces their tendency to form ions and increases their ability to form covalent bonds. Sn acts as a corrosion inhibitor due to the formation of tin oxide. Sn atoms can replace Cu atoms at a substitutional site in the FCC lattice. Tin atoms are randomly distributed throughout the copper lattice. Sn atoms have no preference for the site of grain boundaries or dislocations.

2.5.2. Precipitation hardening

When the Tin content exceeds the solubility limit in Cu, Sn precipitates out of the solution as Cu6Sn5 or Cu3Sn. This precipitate may be in the grain or the grain boundaries. The probability of the location of grain boundaries has been seen more than in the grain, as per the morphological study of samples. In the morphology of LTB9, when Sn% was 14.52%, it was observed that Sn precipitate was seen in ß phase (dendritic form) and δ (lamellar plate form). At the same time, when the percentage of Sn was 12.42 %, dendritic and globular ß phase was seen with Pb precipitate in grains and grain boundaries. If the percentage of Sn is greater than 9%, significant ß phase precipitate was found on grain boundaries. From the morphological study of LTB samples, it is visible that Sn will be available in the α phase for its threshold limit of 8%. The phase-wise morphological analysis in terms of α, ß, and δ for LTB alloy samples is given below in Table 5:

Table 5: Morphological Analysis of LTB Alloys

Sample numbers	Sn wt%	Pb wt%	Zn wt%	Ni wt%	Cu wt%	Existence Of Phase
LTB1	3.5	15.36	0.06	0.9	79.88	α and Pb in grain boundaries
LTB2	5.25	3.13	4.26	2.49	84.69	α and Pb in grain boundaries
LTB3	6.51	4.01	0.92	1.89	86.30	α and Pb in grain boundaries
LTB4	7.79	11.13	0.79	1.32	78.24	α and Pb in grain boundaries
LTB5	9	16	0.11	1.65	72.46	α, ß
LTB6	9.10	10.15	1.33	1.98	77.40	α, ß
LTB7	9.16	4.53	0.98	3.80	80.60	α, ß
LTB8	12.42	12.57	0.24	4.38	70.28	α, ß, and δ
LTB9	14.52	11.85	1.51	3.36	68.24	α, and δ

3. BHN Hardness Model Development

The different compositions of Sn and Pb with Cu, Zn, and Ni were studied for hardness purposes. Zn and Ni were added in minor percentages even in the alloy, so their effect on hardness was seen as minor. So, initially, with three major contributing components like Cu, Pb, and Sn as variables, linear regression analysis was carried out and found an equation for the BHN model as written below:

$$H= C+\text{ß1}X1+\text{ß2}X2+\text{ß3}X3$$

Where H= BHN, C=constant,
X1, X2, and X3 represent Cu, Pb, and Sn, respectively, ß1, ß2, and ß3 their coefficient of wt. Percentage.

∑H=nC +ß1∑X1+ß2 ∑X2+ß3 ∑X3, where n= no of sample hardness

C=H̄ ß1X̄ 1-ß2X̄ -ß3X̄ 3

$$X= \begin{bmatrix} \sum X1^2 & \sum X1X2 & \sum X1X3 \\ \sum X1X2 & \sum X2^2 & \sum X2X3 \\ \sum X1X3 & \sum X2X3 & \sum X3^2 \end{bmatrix}$$

$\sum X1^2 = \sum X1^2 - (\sum X1)^2/n$

∑X1X2=∑X1X2 - ∑X1X2/n

∑X1X3=∑X1X3 - ∑X1X3/n

The same pattern would be followed for the valuation of other rows of matrix X.

$$H= \begin{bmatrix} \sum X1H \\ \sum X2H \\ \sum X3H \end{bmatrix}$$

Where ∑X1H= ∑X1H –(∑X1∑H)/n

The same model would be used to calculate the other row of matrix H.

$[ß] = [X]^{-1} [H]$

After putting the different values of X and H from Table 4 in the above matrix, we get the following matrix:

$$[ß] = \begin{bmatrix} 0.0035 & 0.0014 & 0.0033 \\ 0.0014 & 0.0058 & -0.0002 \\ 0.0033 & -0.0002 & 0.0140 \end{bmatrix} \times \begin{bmatrix} -108 \\ -277 \\ 345 \end{bmatrix}$$

$$= \begin{bmatrix} 0.373 \\ -1.82 \\ 4.52 \end{bmatrix}$$

So, after solving the above matrix equation, the values of ß1, ß2, ß3, and C were found as 0.373, -1.82, 4.52, and 28, respectively. So, based on the above solution, the BHN model equation for LTB alloys can be written as:

BHN =28 +0.37* Cu% +4.52* Sn% -1.82*Pb%

Since Zn works as a softening agent and Ni as a hardening agent, a minor contribution was added on the basis that the virgin hardness of Ni is almost three times greater than that of Zn. So, the ratio between the weighing factors for Ni and Zn on a hit-and-trial basis was decided to be 0.3 and 0.1, respectively. Finally, the BHN model was finalised and written as:

BHN =28 +0.37* Cu% +4.52* Sn% +0.3*Ni% -1.82*Pb%-0.1*Zn%

Samples mean for BHN hardness *of* LTB alloys $X= (\sum H)/n = 637/9 = 79.62$
Standard deviation for the sample's mean $\sigma = \sqrt{\sum(H - X)^2/n} = 18.89$
The population mean based on the above model was calculated for 31 LTB samples with Sn wt. % from 0.5 to 15 at an increment of 0.5 wt.%, and it was found as 85.5.
Population mean $\mu = 85.5$
Due to the sample size being smaller than 30, the authenticity of the population mean would be checked by Student-t-Test as t $(X-\mu)/(\frac{\sigma}{\sqrt{n}})$

After putting the value of variables, the t value comes out as -0.878, which is greater than the left limit -2.841 of the Student-t- t-. Test curve. Hence, the model was authenticated with Student-t-Test with a confidence limit of α=5%, and from the t-test table, the left limit and right limit were taken as -2.841 and +2.841, respectively. It was found that this model will work well within the boundary limit of alloying elements, which are written below:

Boundary Limit of Model: Sn [4.5-13.5%], Pb [1-20%], Zn [0-4.5%], and Ni [0-4.5%]

3.1. Comparison of the hardness of LTB alloys between experimental and model values

The comparison of hardness value based on experimental and Model values is given in Table 6 and a bar chart in Fig. 10.

Table 6: Comparison of Hardness Values for Model and Experimental Basis

Sample	Sn wt%	Pb wt%	Zn wt%	Ni wt%	Cu wt%	Experimental BHN Values	Model BHN Values	Error%	Average error%
LTB1	3.5	15.36	0.06	0.9	79.88	53	45.68	+13.81	
LTB2	5.25	3.13	4.26	2.49	84.69	82	77.68	+5.26	
LTB3	6.51	4.01	0.92	1.89	86.30	78	82.53	-5.80	+9.59/- 9.68
LTB4	7.79	11.13	0.79	1.32	78.24	66	72	-9.00	
LTB5	9	16	0.11	1.65	72.46	57	66.08	-15.92	
LTB6	9.10	10.15	1.33	1.98	77.40	85	79.75	+6.17	

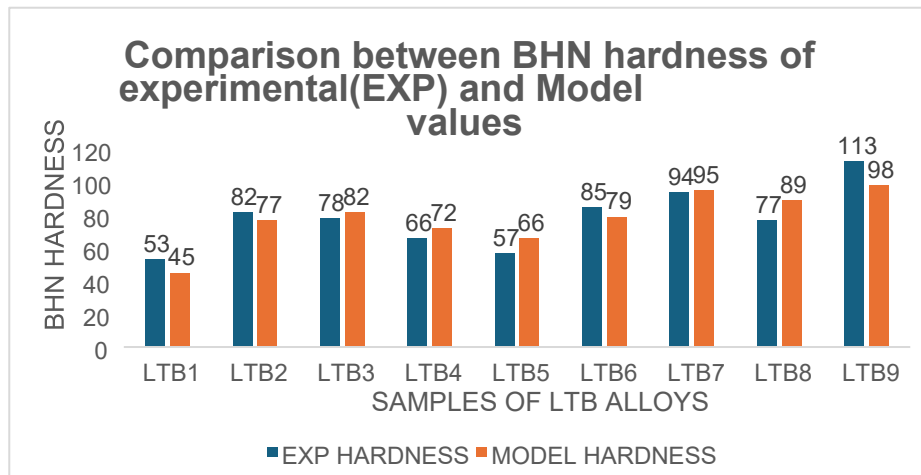|								
LTB7	9.16	4.53	0.98	3.80	80.60	94	95.63	-1.73
LTB8	12.42	12.57	0.24	4.38	70.28	77	89.31	-15.98
LTB9	14.52	11.85	1.51	3.36	68.24	113	98.16	+13.13

Fig. 10: Comparison of BHN Hardness of LTB Alloys between Experimental and Model Values.

From Table 6, it is clear that the above hardness model based on 9 experimental values of hardness for LTB alloys shows the average error of approximately ±9.5, and for a single sample, it has a maximum error limit of +13.81% and a minimum error limit of -15.98%. It seems practical since during BHN measurement by experimentation, variation in the hardness value for the same sample at different places occurs in a wider range. This is the only reason why a minimum of three values of hardness measurement are taken for the same sample at different places, and their average value is considered as the measured hardness value for that sample. The R^2 and RMSE(root mean square error) values were calculated for the model, and they were found as 0.775 and 8.25, respectively, which shows a strong relationship between predicted and experimental hardness.

3.2 Validity testing of the BHN hardness model

The hardness model, which has been developed with the help of experimental values of hardness and regression analysis for different compositions of LTB alloys, was tested with experimental values of other sand-cast samples by the pit furnace named LTB10, LTB11, and LTB12. The wt.% of different compositions of LTB alloys for the above samples is given below in Table 7.

Table 7: Evaluation of Hardness Value by Hardness Model

Samples	Sn wt%	Pb wt%	Zn wt%	Ni wt%	Cu Wt%	Experimental BHN	Model BHN	Error%	Model Average error%
LTB10	5.28	6.88	4.19	2.19	81.35	69.00	69.68	+0.98	
LTB11	6.65	11.85	0.85	1.63	78.68	71.30	66.00	-7.43	±9.5
LTB12	9.55	11.24	0.96	3.34	74.85	74.85	79.30	+5.94	

The above Table 7 depicts that the evaluated values of BHN hardness for samples by the model come out under the model average error percentage of ±9.5. It corroborates the suitability of the applicability of the model for evaluation of BHN hardness of LTB alloys within the working boundary limit of alloying elements as Sn [4.5-13.5%], Pb [1-20%], Zn [0-4.5%], and Ni [0-4.5%].

3.3. Tribological study of LTB alloys

Tribology is the study of knowledge regarding wear, friction, and lubrication of materials. To select the good LTB alloys in the application of bush bearing for the use of submersible pumps, wear and COF tests(three sets of readings and then averaging for each sample for repeatability) were conducted for samples as LTB4, LTB6, LTB10, LTB11, and LTB12 by Pin-on-disc Tribometer, which results are given below in Fig. 11.
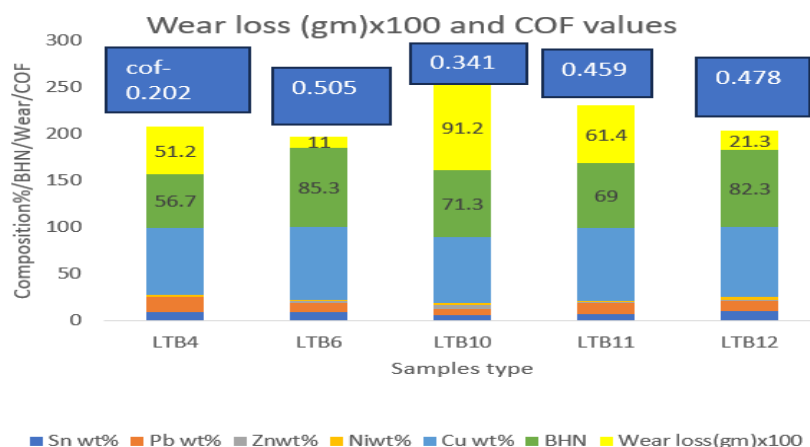

Fig. 11: Wear Loss Values and COF for LTB Alloys.

It is clear from Fig. 11 that as the range of Sn wt% persists in the range of 9-10%, and Pb persists in the range of 10-11%, LTB6 alloy shows the least wear loss of value 11 gm despite of average COF higher value of 0.505. This might be happening due to the formation of the alpha phase of copper and the beta phase of Sn in LTB alloys. Sn and Cu have almost similar atomic size, hence leading to mutual solubility to form a homogeneous alloy. Their similar electronegativity promotes covalent bonding, which gives higher strength and hardness than pure copper, and enhanced corrosion resistance due to protective tin oxide. Tin dissolves in the copper matrix, causing lattice distortion that increases hardness and wear resistance. Cu-Sn precipitate can act as an obstacle to dislocation movement, hence higher wear resistance and high COF. In copper-Pb solution, copper and Pb have extremely different atomic sizes, making it difficult for atom of Pb atom to substitute copper atom. So Pb typically nucleates at grain boundaries, triple points, dislocations, and defects. During the wear test, it was observed that Pb is acting as a solid lubricant in Cu-Sn hard matrix, hence despite of higher COF value of 0.505, BHN of 85.3, the least wear loss value is occurring. Although for the same wt% 9-10% of Sn, if the Pb value is higher than 10%, Pb acts as a softer agent, hence a lesser average COF and higher wear loss is obtained. Since the LTB6 has a lower wear loss, its SEM-EDS analysis was carried out on a JSM-6490LV microscope with an EDS setup. The morphological image of LTB6 before wear and after wear test by SEM-EDS is given below in Figs 12,13,14,15,16,17,18, and 19.
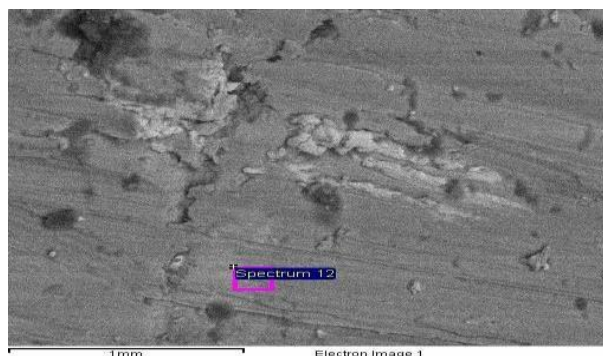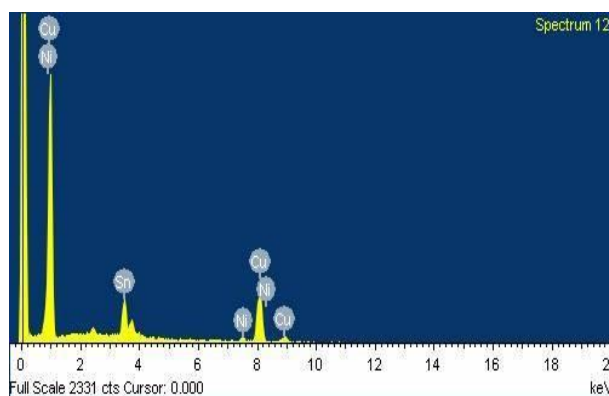

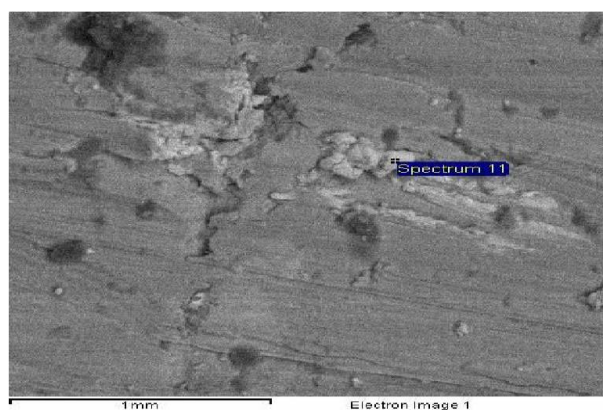**Fig 12:** SEM of LTB 6 (Before Wear).

Fig. 13: EDS of LTB6 (Before Wear).

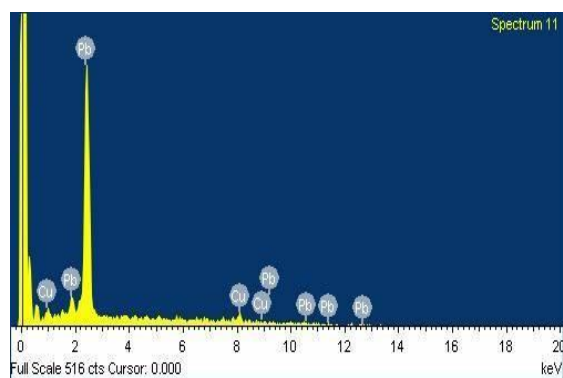**Fig. 14:** SEM of LTB 6(Before Wear)

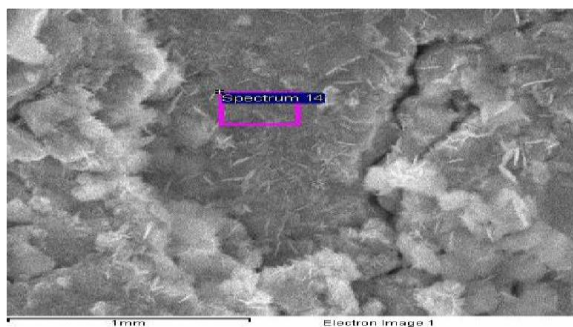**Fig. 15:** EDS of LTB 6(Before Wear).

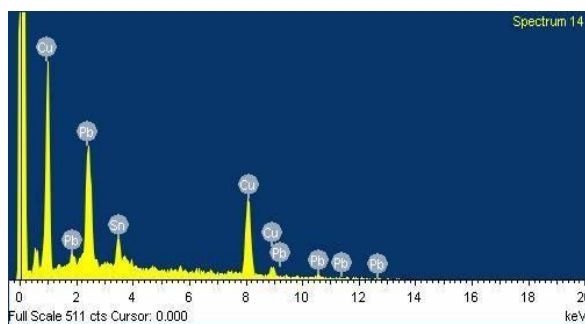**Fig. 16:** SEM of LTB 6(After Wear).

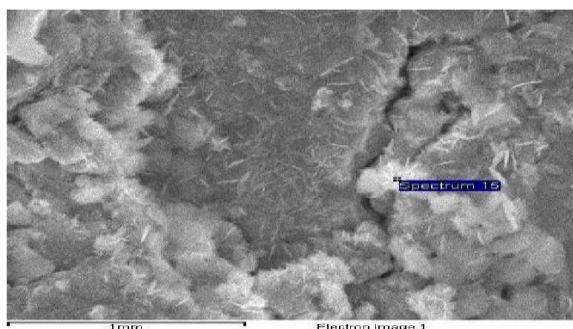**Fig. 17:** EDS of LTB6(After Wear).
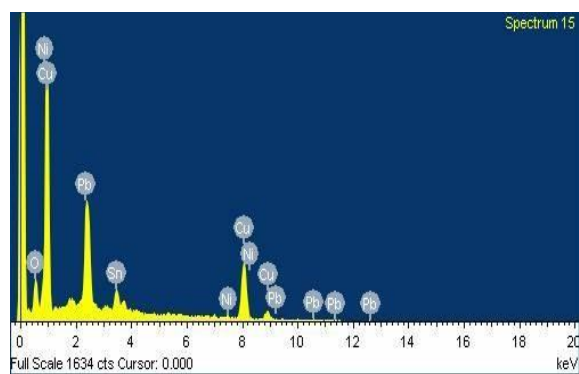

Fig 18: SEM of LTB6 (After Wear).

Fig. 19: EDS of LTB6 (After Wear).

The SEM analysis of LTB6 clearly depicts that Pb is not soluble in the Cu matrix; hence, it was nucleated separately at the grain boundaries of the Cu matrix. The white part of the image in Fig. 12 indicates the presence of Pb, which is validated by the EDS picture in Fig. 13. Similarly, the grey part of the image in Fig.14 indicates solid solution of Sn, Zn and Ni in the Cu matrix, and the same is authenticated by the EDS picture in Fig. 15. After wear test of LTB6, the worn-out surface of it was analyzed by SEM-EDS which has been shown in Fig 16,17,18 and 19. The SEM analysis of the worn-out surface clearly indicates that smearing of Pb has occurred throughout the Cu matrix in the form of particulate fibres, which contributed to solid lubrication during the mating of the two surfaces in motion. This may be the one reason why, despite the higher average COF of LTB6, the lowest wear loss occurs.

3.4. Results and discussion

The hardness results obtained for LTB alloys, as mentioned in Table 4, clearly depict that as the wt.% of Sn increases in the alloy, it plays the role of a hardness enhancer, while Pb acts as a hardness reducer. It might be occurring due to the larger atomic size of Sn than Cu atomic size in the solid solution, and because of this, Sn creates the lattice distortion, which impedes the dislocation movement. Due to the larger atomic size of Pb and low solubility in Cu, it precipitates in grain boundaries as globules or particles, as shown in Figs 3,4, and 5. Pb has a high enchantment for grain boundaries, where it can segregate and form globules. This might have happened in the case of Pb because grain boundaries provide a high-energy point for Pb atoms to accumulate. Sn presence seems in α phase up to 8 wt.% in the alloy, and with this, Pb presence in grain boundaries. For 9-12 wt.% of Sn in the alloy, it occurs in the ß phase with Pb again at grain boundaries. Furthermore, enhancement of Sn wt.% as 12-14%, Sn presence seems in α, ß, and δ phases with Pb in grain boundaries and lattice. Ni and Zn work as alpha-phase stabilisers, while Pb works as a beta and delta-phase reducer. The morphology of Sn in Cu alloy was seen as globular, rod-like, and plate-like. Pb reacts with O_2 to form PbO_2, which acts as a lubricant. The developed hardness model for LTB alloys is widely applicable for finding out their BHN values within the prescribed limit of wt.% of alloying elements, with an average error of ± 9.5. It has been validated with another casted LTB alloys and found to provide experimental BHN values that were very close to model hardness values as per Table 7. Hence, this BHN hardness model would be useful for evaluating the BHN of LTB alloys. Similarly morphological study of LTB alloys shall be beneficial for researchers to assess the effect of hardness on different phases of Sn for wear and coefficient of friction evaluation. In LTB alloys, due to the formation of Cu-Sn compound as a solid solution for Sn wt% in the range of 9-10, % highest BHN values of 85.3 were observed, hence the lowest wear loss of value 11 gm, provided that 10% of Pb has acted as solid lubrication. The highest COF value, 0.505, might be occurring due to the highest hardness of LTB6, and due to this, harder delaminated debris creates abrasion, hence higher COF.

4. Conclusion

1) Morphological studies of LTB alloys show that Sn appears as a solid solution in copper for its threshold limit of 8% wt.. in composition. Between 8-9% wt. of Sn in the composition of LTB alloys, Sn appears as a solid solution with copper, with the inception of Sn as precipitate in the supersaturated solid solution. As wt. Percentage of Sn increases beyond 9%, Sn appears as the ß phase in grain boundaries and as the δ phase for Sn% higher than 12%.
2) The experimental values of hardness show that as the Sn% increases, Hardness increases with Pb as a softening agent. The minimum BHN for LTB 1 was found as 53, and the maximum for LTB9 as 113 experimentally. The developed BHN model based on linear regression analysis was proven to work well within the boundary limit of Sn [4.5-13.5%], Pb [1- 20%], Zn [0- 4.5%], and Ni [0-4.5%] with an average error of ± 9.5.
3) Wear, and COF test of LTB alloys conclude that the least wear loss (11 g) or in other terms 3.89×10^{-3} g/m and the highest COF value (0.505) were observed for LTB6 alloy, which contains Sn-9.1%, Pb-10.15%, Zn- 1.33%, Ni-1.98% and balance copper.

Acknowledgement

Authors Contribution

The first author's- Ram Dhani Chauhan, contribution is 75% which includes conception, design of study, acquisition of data, analysis and interpretation of data, and drafting of article, and the second author's- Dr Prem Kumar Bharti, contribution is 25% which includes review of article and addition of his views at the required places.

Declaration

1) Ethical Approval: Not applicable.
2) Clinical Trial No: Not Applicable.
3) Consent to participate: Not applicable.
4) Consent to Publication: Not applicable.
5) Funding: "not applicable".

Competing of Interest

There is no conflict of interest between the authors. The author and co-author have no competing interests for their employment, consultancies, stock ownership, honoraria, paid expert testimony, patent applications/registrations, etc.

Data Availability

Yes, and all the data generated or analysed during this study are included in this article.

References

[1] Zaghloul MMY, Steel Karen, Heitzmann, T Michael: Wear behaviour of polymeric materials reinforced with man-made fibres: a comprehensive review about fibre volume fraction influence on wear performance. Journal of Reinforced Plastics and Composites; 41 (5-6), (2021). https://doi.org/10.1177/07316844211051733.

[2] Zaghloul MMY, Steel K, Veidt M, Heitzmann MT: Mechanical and tribological performances of thermoplastic polymers reinforced with glass fibres at variable fibre volume fractions. Polymers;15, 694, (2023). https://doi.org/10.3390/polym15030694.

[3] Zaghloul, M.M.Y.: Effect of Nano Particles on the Mechanical Properties of Thermosetting Polymeric Materials Reinforced with Glass Fibers, MSc Thesis. Faculty of Engineering, Alexandria University, (2018).

[4] Zaghloul MMY, Steel K, Veidt M, Heitzmann MT: Influence of counter-face grit size and lubricant on the abrasive wear behaviour of thermoplastic polymers reinforced with glass fibres. Tribol Lett;71, 102, (2023). https://doi.org/10.1007/s11249-023-01774-9.

[5] Zaghloul Yousry Mahmoud Moustafa, Steel. Karen, Veidt, Martin: Heitzmann, Michael T. H: Assessment of the tribological performance of glass fibre reinforced polyamide 6 under harsh abrasive environments, Tribology International, 191, pp. 1- 20, (2024). https://doi.org/10.1016/j.triboint.2023.109059.

[6] Cartledge HCY, Baillie CA: Effects of crystallinity, transcrystallinity and crystal phases of GF/PA on friction and wear mechanisms. Journal of Materials Sci; 37: 3005– 22, (2002). https://doi.org/10.1023/A:1016081317081.

[7] Deyong, L., Tremblay, R., and Angers, R.: Microstructural and mechanical properties of rapidly solidified Cu-Ni-Sn alloys. *Materials Science and Engineering A*, 124(2), 223-231, (1990). https://doi.org/10.1016/0921-5093(90)90152-S.

[8] Rahul Gupta, Sanjay Srivastava, Preetham Kumar GV, and Sanjay K Penthi: Investigation of mechanical properties, microstructure, and wear rate of high leaded Tin bronze after multidirectional forging; Procedia Material Science 5, 10811089, (2004). https://doi.org/10.1016/j.mspro.2014.07.401.

[9] Xiang, J.SadaH; Xang, X, MiuraH, Sakai T: Ultrafine grain development in an A231 magnesium alloy during multidirectional forging under decreasing temperature condition; Mate Cai, C; Evaluation of the friction and wear properties of PEI composites filled with glass and carbon fibre; Advanced material research, vol 299300, pp 21-24, (2011). https://doi.org/10.4028/www.scientific.net/AMR.299-300.21.

[10] Prasad, B.K: Sliding wear behaviour of bronzes under varying material composition, microstructure and test condition, wear 257, 110-123, (2004). https://doi.org/10.1016/j.wear.2003.10.021.

[11] Pathak, J.P; Tewari, SN: Mechanical and wear properties of copper-lead bearing alloys; wear 155,37-47, (1992). https://doi.org/10.1016/0043-1648(92)90107-J.

[12] Gao, L.L; Cheng, X.H: Effect of ECAE on microstructure and tribological properties of CU-10Al-4Fe alloy, tribology letter 27, 221-225. (2007). https://doi.org/10.1007/s11249-007-9228-7.

[13] Moustafa. S; EI-Badry. S, Sanod.A and Kieack. B: Friction and wear of copper graphite composite made with Cu coated and uncoated graphite powder; Wear, vol.253, pp 699-710, (2002). https://doi.org/10.1016/S0043-1648(02)00038-8.

[14] Rajkumar. K and Arvindan. S: Tribology behaviour of microwave processed copper nano graphite composite; Wear; vol. 265, pp 417-421 (2008).

[15] S. ILANGOVAN, R.: Effect of Tin hardness, wear rate and coefficient of friction of cast Cu-Ni-Sn alloys, Journal of Engineering Science and Technology Vol-8 no1, 34-35, (2003).

[16] Zhang, S-Z, Jiang B.H and Ding, W: Wear of Cu-15Ni-8 Sn spinodal alloy, wear,264(3-4),199-203, (2008). https://doi.org/10.1016/j.wear.2007.03.003.

[17] Singh, J.B, Cai, Wand Bellon P.: Dry sliding of Cu-15Ni-8Sn bronze wear behaviour and microstructure, wear 263(1-6),830-841, (2007). https://doi.org/10.1016/j.wear.2007.01.061.

[18] Seah,K.H, Hemanth,J, Sharma, S.C: The Effect of Solidification Rate on Morphology Microstructures and Mechanical Properties of 80%Cu-20%Sn Bronze Alloys *Journal of Material Science* 33: 23-28, (1998).

[19] Hemanth Joel: Effects of cooling rate on dendrite arm spacing and hardness of aluminium–silicon alloy, Journal of Materials and Design 21: 1-8 (2000). https://doi.org/10.1016/S0261-3069(99)00052-7.

[20] Sugita.Gede.I Ketut; Soekrisno.R;Maisa.I.Made and Suitno: The Effect of Solidification Rate on Marphology Microstructure and Mechanical properties of 80% Cu-20% Sn Bronze alloys; Material Science Research of India, Vol 7(1), 59-66 (2010). https://doi.org/10.13005/msri/070106.

[21] Brush Wellman: Strengthening Mechanisms. *Technical Tidbits*, 3, 1-2, (2001).

[22] H. Liu, F. Xue, J. Bai, Y. Sun: Effect of heat treatments on the microstructure and mechanical properties of an extruded Mg95.5Y3Zn1.5 alloy Mater. Sci. Eng. A, 585, pp. 261-267, (2013). https://doi.org/10.1016/j.msea.2013.07.025.

[23] H.W. Richardson, Handbook of Copper Compounds and Applications, 14, no. 3. (2000).

[24] K.Manu, J. Jezierski, M.R.S. Ganesh, K.V. Shankar, S.A. Narayanan: Titanium in cast cu-sn alloys—a review Materials, 14 (16) (2021). https://doi.org/10.3390/ma14164587.

[25] Chauhan RD; Bharti.PK: A review of Tribological excellence of Bronze Alloys; Discover of Applied Science; Volume 7, 238, (2025). https://doi.org/10.1007/s42452-025-06610-4.

[26] Wang Xiaoming , TangBoen , WangLinlin , WangDongyun 1 DongWeiping, GLi Xipig : Microstructure, Microhardness and Tribological Properties of Bronze–Steel Bimetallic Composite Produced by Vacuum Diffusion Welding; Materials , 15(4), 1588,(2022). https://doi.org/10.3390/ma15041588.

[27] A. Sirinaidu. D, D. RamaJogi: Experimental evaluation in the properties of various Tin Bronze, IJLTEMAS, Volume iv, Issue vi, June (2015).